RESEARCH ARTICLE

Malic enzyme 1 induces epithelial–mesenchymal transition and indicates poor prognosis in hepatocellular carcinoma

**Duo Wen · Dongli Liu · Jun Tang · Lili Dong · Yang Liu ·
Zhonghua Tao · Jinliang Wan · Dongmei Gao · Lu Wang ·
Huichuan Sun · Jia Fan · Weizhong Wu**

Abstract Malic enzyme 1 (ME1) links the glycolytic and citric acid cycles and is important for NADPH production, glutamine metabolism, and lipogenesis. Recently, its deregulation has been implicated in the progression of various cancers. However, the role of ME1 in the progression of hepatocellular carcinoma (HCC) remains unclear. In this study, we utilized short hairpin RNA-mediated gene silencing to investigate the biological effects of ME1 depletion in HCC and determined its prognostic significance in HCC. ME1 expression was examined by real-time (RT)-PCR and Western blot using five HCC cell lines and one normal liver cell line. We used polyethylenimine nanoparticles to deliver a short hairpin RNA to induce cessation of ME1 expression in HCC cells. Changes in NADPH production and reactive oxygen species (ROS) production were studied. Metastatic potentials of HCC cells were evaluated in vitro. Furthermore, we evaluated the protein level of ME1 in para-tumor and cancerous tissues of 65 HCC patients with detailed clinical, pathological, and clinical follow-up data. Patients' survivals were further assessed as well. Upregulated ME1 expression was observed in HCC cell lines. Downregulation of ME1 attenuated NADPH production and stimulated ROS production. Silencing ME1 was noted to inhibit migratory and invasive properties of HCC cells by inducing the E-cadherin expression and decreasing of N-cadherin and vimentin expression in a ROS-dependent pathway. Overexpression of ME1 was observed in a major fraction of HCC samples. Higher level of ME1 in tumors was significantly associated with reduced overall survival (Kaplan–Meier analysis, $P=0.024$) and reduced progression-free survival (Kaplan–Meier analysis, $P=0.011$). Inhibition of

Duo Wen and Dongli Liu contributed equally to this work.

D. Wen · D. Liu · J. Tang · L. Dong · Y. Liu · Z. Tao · J. Wan ·
D. Gao · L. Wang · H. Sun · J. Fan · W. Wu (✉)
Liver Cancer Institute, Zhongshan Hospital, Fudan University, 180
Fenglin Road, Shanghai 2000032, China
e-mail: drwzwu2015@163.com

D. Wen
e-mail: wenduo@outlook.com

D. Liu
e-mail: loveliudongli@163.com

J. Tang
e-mail: judytangjun@163.com

L. Dong
e-mail: dong2044@sohu.com

Y. Liu
e-mail: lizzy0714@126.com

Z. Tao
e-mail: drtaozhh@126.com

J. Wan
e-mail: wanjinliang01@163.com

D. Gao
e-mail: gao.dongmei@zs-hospital.sh.cn

L. Wang
e-mail: wang.lu@zs-hospital.sh.cn

H. Sun
e-mail: sun.huichuan@zs-hospital.sh.cn

J. Fan
e-mail: jiafan99@yahoo.com

D. Wen · D. Liu · J. Tang · L. Dong · Y. Liu · Z. Tao · J. Wan ·
D. Gao · L. Wang · H. Sun · J. Fan · W. Wu
Key Laboratory of Carcinogenesis and Cancer Invasion, Ministry of
Education, Shanghai 200032, China

J. Fan
Institute of Biomedical Sciences, Fudan University,
Shanghai 200032, China

ME1 expression decreases HCC metastasis via suppression of epithelial–mesenchymal transition (EMT) processes in ROS-induced pathways. ME1 overexpression associates with unfavorable prognoses in patients with HCC, suggesting that ME1 is a poor prognostic predictor of hepatocellular carcinoma.

Introduction

Hepatocellular carcinoma (HCC) is the third leading cause of cancer-related mortality, with nearly 600,000 deaths occurring worldwide each year [1]. Although resection is considered a potentially curative treatment for HCC patients, metastasis has still been a bottleneck troublesome in HCC therapy and prognosis management [2].

Cancer cells reprogram their metabolism to support increased proliferation through via increased glycolysis and biosynthetic activities, known as the "Warburg effect" [3]. Metabolic reprogramming is now considered to be a central mechanism of tumor progression, not merely being one of many features present in changes particular to tumor cells [4, 5]. Several metabolism proteins related to cellular metabolisms and signaling pathways have been described to correlate with metastatic relapses and poor prognosis in cancer patients; additionally, some metabolism-regulated genes related to metabolic anomalies have been validated via basic and clinical studies [6–8]. However, mechanisms of tumor metastasis have not been fully elucidated, especially in HCC. Metabolic reprogramming in cancer cells presents to be an important potential mechanism in tumor progression and metastasis.

Malic enzyme 1 (ME1) is a cytosolic protein with its gene located at on chromosome 6q12. ME1 links the glycolytic and citric acid cycles and is important for NADPH production, glutamine metabolism, and lipogenesis [9, 10]. A survey of public gene expression databases (http://www.oncomine.org) revealed that ME1 expression was significantly upregulated in a variety of human cancers, such as nasopharyngeal carcinoma, breast cancer, and neuroblastoma [11]. The enzyme is noted for interaction with p53 and promotes p53-dependent tumor progression and metastasis [11]. Silencing ME1 attenuates migratory and invasive abilities in nasopharyngeal carcinoma [12]. All clearly shows that ME1 plays an important role in the regulation of tumor progression and metastasis.

However, ME1's function in regulating HCC metastasis as well as its clinicopathological significance remains largely unexplored to date. In this study, we identify the pivotal roles of ME1 in promoting HCC metastasis as well as its significant value in HCC patients. ME1 represents a novel biomarker and therapeutic target for HCC.

Materials and methods

Cell lines

MHCC97L, MHCC97H, HCCLM3 (human HCC cell lines with different metastatic potentials established at the Liver Cancer Institute, Zhong Shan Hospital, Fudan University, Shanghai, China) [13, 14], HepG2, Huh7 (two low metastatic human HCC cell lines; American Type Culture Collection), and one immortalized normal liver cell lines L02 were used in this study [15, 16]. L02, HepG2, and Huh7 cells were purchased from the Shanghai Cell Bank, Chinese Academy of Sciences. MHCC97L, MHCC97H, and HCCLM3 were established by our institute, Zhongshan Hospital, Fudan University, Shanghai, China [17–19]. All these cells were cultured under standard conditions: DMEM (Gibco, Inc.) supplemented with 10 % FBS (Gibco, Inc.), and routinely maintained in a humidified incubator at 5 % CO^2 at 37 °C [20].

shRNA plasmid and transfection

The functions of ME1 in HCC cells were evaluated via short hairpin RNA (shRNA) plasmids targeting ME1. Three sequences of shRNA-targeting ME1 were designed and cloned into a pLKO.1 TRC cloning vector: 5′-GGGCATATTGCTTC AGTTCTTCAAGAGAGAACTGAAGCAATATGCCC-3′ for sh#1; 5′-GAGAGACAGCAATTGAACATTCAAGAGA TGTTCAATTGCTATCTCTC-3′ for sh#2; 5′-GCGAGATA TTGCGAGAGAAGGTTCTAGATCTATATCGAAT-3′ for sh#3, while the sequence of scrambled shRNA was 5′-TAGGATTCGTTCAAGAGACGAATCCTACAAAGCG CGC-3′ and used to generate a negative-control plasmid. The knockdown efficacy was evaluated by Western blot. All these plasmids were transfected into HCC cells using Lipofectamine 2000 in accordance to the product manual (Invitrogen, Inc.).

RNA extraction and real-time PCR assays for mRNA detection

Total RNA was extracted from cultured cells with TRIzol Reagent (Invitrogen, Inc.). The quality and integrity of RNA was evaluated via A260/A280 ratio and 18 s/28 s band by agarose electrophoresis. 1 μg of total RNA was used for first-strand DNA synthesis employing a PrimeScript™ RT reagent kit (Takara Bio, Inc., Japan). Real-time PCR was performed in triplicate by according to the SYBR Green PCR

method, with a SYBR Premix Ex Taq™ kit (Takara Bio, Inc., Japan) and in accordance with the manufacturer's instructions. The primers for the interested genes (ME1, E/N-cadherin, vimentin) were synthesized by Sangon Company (Sangon Biotech Co., Ltd., Shanghai, China), as follows: 5′-CTTCAT GCCTGACTGATAT-3′ (forward) and 5′-GACGTCTCAG GACTTACG-3′ (reverse) for ME1; 5′-CTGCAGGTCTCA TCATGGA-3′ (forward) and 5′-ACCTGTAGACCTCGGC ACTG-3′ (reverse) for E-cadherin; 5′-CCGTGAATGGGC AGATCACT-3′ (forward) and 5′-TAGGCGGGATTCCATT GTCA-3′ (reverse) for N-cadherin; 5′-GAGTCCACTGAG TACCGGAGAC-3′ (forward) and 5′-TGTAGGTGGCAA TCTCAATGTC-3′ (reverse) for vimentin; 5′-CACCATGA AGATCAAGATCATTGC-3′ (forward) and 5′-GGCCGG ACTCATCGTACTCCTGC-3′ (reverse) for glyceraldehyde 3-phosphate dehydrogenase (GAPDH). The GAPDH was used as internal control for messenger RNA (mRNA) assays. The threshold cycle (Ct) values were analyzed using the comparative Ct ($-\Delta$Ct) method. The level of targets was obtained by normalizing to the endogenous reference and relative to a control.

Protein levels detected by Western blot analysis

Lysates were obtained from 1×10^6 cultured cells with a mixture of ProteoJET Mammalian Cell Lysis Reagent (Fermentas, Inc.); phenylmethanesulfonyl fluoride (Roche, Inc.); and PhosSTOP (Roche, Inc.). About 20 μg protein was extracted from each sample, separated by 10 % sodium dodecyl sulfate-polyacrylamide gel electrophoresis (SDS-PAGE). After being blocked in 5 % nonfat milk, the interested protein was probed with antibody either against human ME1 (1:1000, Abcam), E-cadherin (1:1000, Cell Signaling Technology), vimentin (1:500; Bioworld Technology, Inc.), or GAPDH (1:3000; Abcam); then incubated with goat anti-rabbit or anti-mouse IgG (1:10,000 for both; Jackson ImmunoResearch Laboratories); and detected with enhanced chemiluminescence reagents (Thermo Fisher Scientific). The bands were visualized using 1-stepTM NBT/BCIP reagents (Thermo Fisher Scientific, Rockford, IL, USA) and detected by the Alpha Imager (Alpha Innotech, San Leandro, CA, USA) [20, 21].

In vitro migration and invasion assays

Cell migration and invasion were analyzed by a Transwell™ Permeable Supports system with 8-μm pores (Corning, Inc.) according to the manufacturer's instructions. MHCC97H and HCCLM3 were transfected with a total of 80 nM ME1 shRNA or scrambled shRNA (80 nM) for 60 h using Lipofectamine 2000 before plating, respectively. For migration assays, 5×10^4 cells were seeded into the Matrigel-uncoated upper insert at 24 wells in medium supplemented with 1 % serum. Medium containing 10 % serum was added to the well as

a chemoattractant. Following a culture of 36 h, non-invading cells were removed from the upper surface by wiping with a cotton swab. For invasion assays, 1.0×10^5 cells were seeded into the Matrigel-coated upper insert at 24 wells in medium supplemented with 1 % serum. Medium containing 10 % serum was added to the well as a chemoattractant. Following a culture of 48 h, non-invading cells were removed from the upper surface by wiping with a cotton swab. Then, the membranes were fixed with 4 % formaldehyde for 15 min at room temperature. The invading cells were stained with Giemsa (Sigma, Munich, Germany) for 25 min, and their numbers in 10 fields of each triplicate filter were analyzed by inverted microscope. For cellular morphology studies, 1.0×10^5 cells were seeded into the 6-wells in medium supplement with 7 % serum, with or without N-acetyl-L-cysteine (NAC, Sigma, Inc.) 10 mmol/L for 12 h. Following a culture of 60 h, cells were washed twice in phosphate-buffered saline (PBS) and analyzed by inverted microscope [20, 21].

NADPH quantification

NADPH quantification of MHCC97H and HCCLM3 cells was performed using an NADP$^+$/NADPH quantification kit (Biovision, Inc.) in accordance with the manufacturer's protocols. Pellet 4×10^6 cells after washing with cold PBS for each assay in a microcentrifuge tube (2000 rpm for 5 min). Lyse the cells with 800 μl of NADP/NADPH Extraction Buffer in a microfuge tube and keep on ice for 10 min. Spin down at 10, 000×g for 10 min, and collect the supernatant. Transfer the extracted NADP/NADPH solution into a new labeled tube. To detect total NADP/NADPH (NADPt), transfer 50 μl of extracted samples into labeled 96-well plate in duplicates. Prepare a NADP Cycling Mix for each reaction: NADP Cycling Buffer Mix: 98 μl; NADP Cycling Enzyme Mix: 2 μl. Mix well and add 100 μl of the mix into each well, mix well. Incubate the plate at room temperature for 5 min to convert NADP to NADPH. Add 10 μl NADPH developer into each well. Let the reaction develop for 1 h. Read the plate at OD450 nm [22].

Determination of ROS generation

Changes in intracellular reactive oxygen species (ROS) levels were determined by measuring the oxidative conversion of cell permeable 2′,7′-dichlorofluorescein diacetate (DCFH-DA) to fluorescent dichlorofluorescein (DCF) in FACS Calibur flow cytometry system (BD Biosciences, Inc.). After treatment with ME1 shRNA, with or without N-acetyl-L-cysteine (NAC, Sigma, Inc.) 10 mmol/L for 12 h, cells were washed twice in phosphate-buffered saline (PBS). For each sample 1×10^6 cells were then incubated with 10 μmol/ LDCFH-DA at 37 °C for 30 min according to the manufacturer's instructions, washed twice with PBS and resuspended

for detection of ROS accumulation using the FACSCalibur flow cytometry system (BD Biosciences, Inc) at an excitation wavelength of 488 nm and an emission wavelength of 538 nm [23].
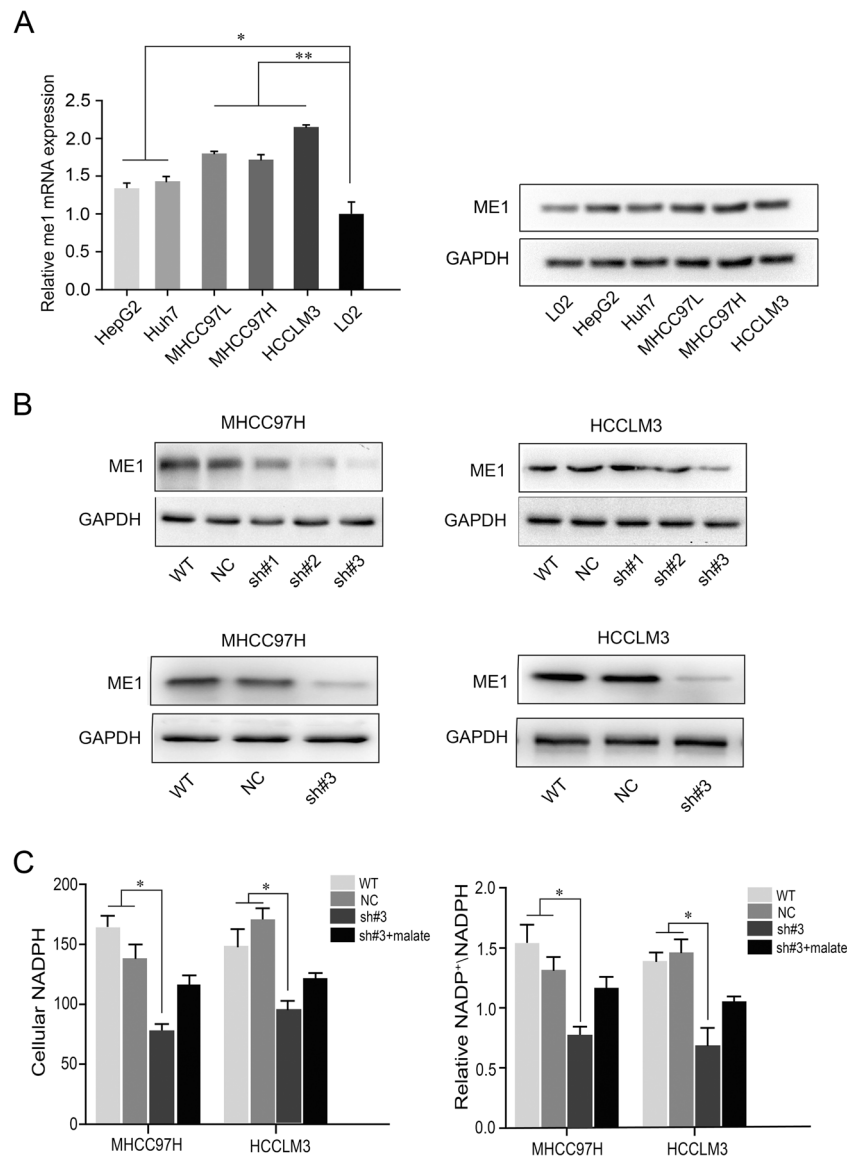
Patient selection and evaluation

Sixty-five patients with primary hepatocellular carcinoma (HCC) who underwent curative liver resection with pathologically confirmed were randomly enrolled. Tumor stage was determined according to the TNM classification system (2002 International Union against Cancer). All procedures were approved by the Zhongshan Hospital Research Ethics Committee. Informed consent was obtained from each patient according to regulations set forth by the Ethics Committee.

Immunohistochemical assays

Immunohistochemistry for the target molecules was performed on single serial sections made from surgical samples. The slides were probed with a primary antibody against ME1 (1:200; Abcam, Inc.), and then incubated with horseradish peroxidase-conjugated IgG (1:500; Invitrogen, Inc.), and the proteins in situ were visualized with 3,3′-diaminobenzidine. The intensity of positive staining was measured with integrated optical density (IOD) as previously described [24]. The intensity of ME1 was classified as either high- or low-expression [median value of IOD (mIOD) was used as the cutoff value; ME1 high-expression IOD>mIOD, and ME1 low-expression IOD<mIOD]. When cut off with mIOD, patients with ME1 density over mIOD were categorized into ME1 high-expression group and patients with ME1 density less than mIOD were categorized into ME1 low-expression group.

Fig. 1 Relative ME1 expression and NADPH quantification. **a** Real-time PCR analysis to quantify the endogenous levels of ME1 in HepG2, Huh7, MHCC97L, MHCC97H, HCCLM3, and L02 cells. β-actin was included as a loading control and all data were normalized to the level of L02 cells (*left*). Western blot analysis to evaluate the protein levels of ME1 in HepG2, Huh7, MHCC97L, MHCC97H, HCCLM3 and L02 cells (*right*). GAPDH was used as a loading control. **b** Western blot analysis of ME1 in wild-type (*WT*), control (*NC*), and knockdown (*sh#1, sh#2, sh#3*) cells. **c** Cells were collected to measure NADPH concentration. WT, NC, sh#3, and malate were defined as wild-type, negative-control scramble shRNA transfected, dimethyl L-malate, respectively. Data are mean±SEM (*n*=3) and are representative of three independent experiments. Statistical analysis by paired *t* test (*$*P<0.05$; **$P<0.01$)

Statistical analyses

Survival was calculated from the initial of interventional therapy to death or cessation of clinical follow-ups. Data were analyzed using GraphPad Prism 5 software or Statistical Program for Social Sciences software 19.0 (SPSS, IBM). Quantitative variables were expressed as means±SD and analyzed by one-way ANOVA, Student's *t* test, Kruskal–Wallis test, or Mann–Whitney *U* test. Qualitative variables were compared using Pearson chi-squared test or Fisher exact test. Overall survival was estimated using Kaplan–Meier methods, and the difference in survival was evaluated by log-rank tests. Cox proportional hazards regression was used to detect predictors of survival. Results were considered statistically significant at $P < 0.05$.

Results

ME1 overexpression in HCC cell lines

We chose five representative liver cancer cell lines, HepG2, Huh7, HCCLM3, MHCC97H, MHCC97L, and one human hepatic cell line, L02, to evaluate ME1 mRNA and protein levels. Levels of ME1 transcripts in HepG2, Huh7, HCCLM3, MHCC97L, and MHCC97H lines were significantly increased in comparison with the normal liver cell line L02, as shown in Fig. 1a. Western blot assays further confirmed the significance of unregulated ME1 expression in all HCC cell lines. Of the five HCC cell lines, MHCC97H and HCCLM3 were noted to have the highest levels of ME1

Fig. 2 ROS quantification, migration, and invasion assays. **a** WT, NC, sh#3, sh#3+malate, and sh#3+NAC cells were collected to measure reactive oxygen species (ROS) concentration. **b** Motility assays of MHCC97H and HCCLM3 cells with indicated treatment. **c** Invasion assays of MHCC97H and HCCLM3 cells with indicated treatment (*n*=3). Data are mean±SEM and are representative of three independent experiments. Statistical analysis by paired *t* test (*$P < 0.05$)
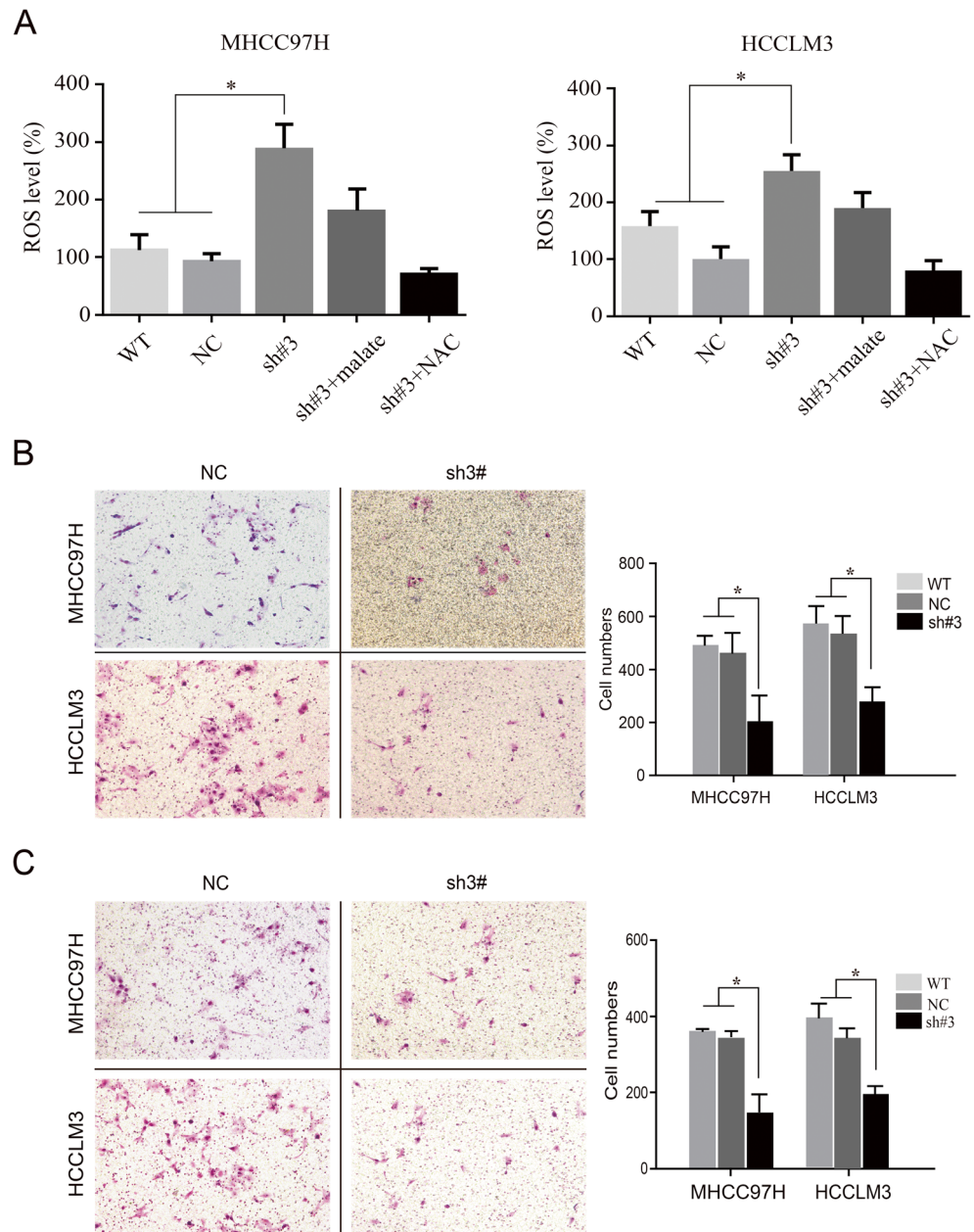
expression and thus were selected for investigating the role of ME1 in HCC.

Impaired NADPH production and stimulated ROS generation in ME1-repressed cells

Tumor cells usually take up excessive nutrients and produce numerous metabolites such as NADPH and ATP, etc. for bioenergetics needs [25]. Due to the pivotal role in cell glycolysis and NADPH production, we wondered whether NADPH production would be modulated by ME1 in HCC cell lines. Three

shRNA plasmids targeting ME1 were constructed and transfected into MHCC97H and HCCLM3 cells. The third one (sh#3) was found to have the highest knockdown efficiency in three tested shRNAs, as shown in Fig. 1b. And the NADPH concentration in MHCC97H and HCCLM3 cells was indeed decreased in both ME1-repressed MHCC97H and HCCLM3 cells, as shown in Fig. 1c. As the direct role of NADPH on the homeostasis of cytosolic redox state which might be destroyed by an accumulation of intracellular ROS level [26], we further investigated whether or not the levels of ROS was increased after ME1 depletion. A fluorescent

Fig. 3 The morphological changes of HCC cells and relative expression of EMT markers. **a, c** Images showing the morphological changes of MHCC97H and HCCLM3; *Bars* 100 μm. **b, d** Western blot analysis to evaluate the protein levels of ME1, E-cadherin, N-cadherin, and vimentin in MHCC97H and HCCLM3. GAPDH was used as a loading control. Real-time PCR analysis to quantify the level of E-cadherin, N-cadherin, and vimentin in MHCC97H and HCCLM3 cells. β-actin was included as a loading control and all data were normalized by NC cells. Data are mean±SEM (n=3) and are representative of three independent experiments. Statistical analysis by paired t test (*P<0.05)
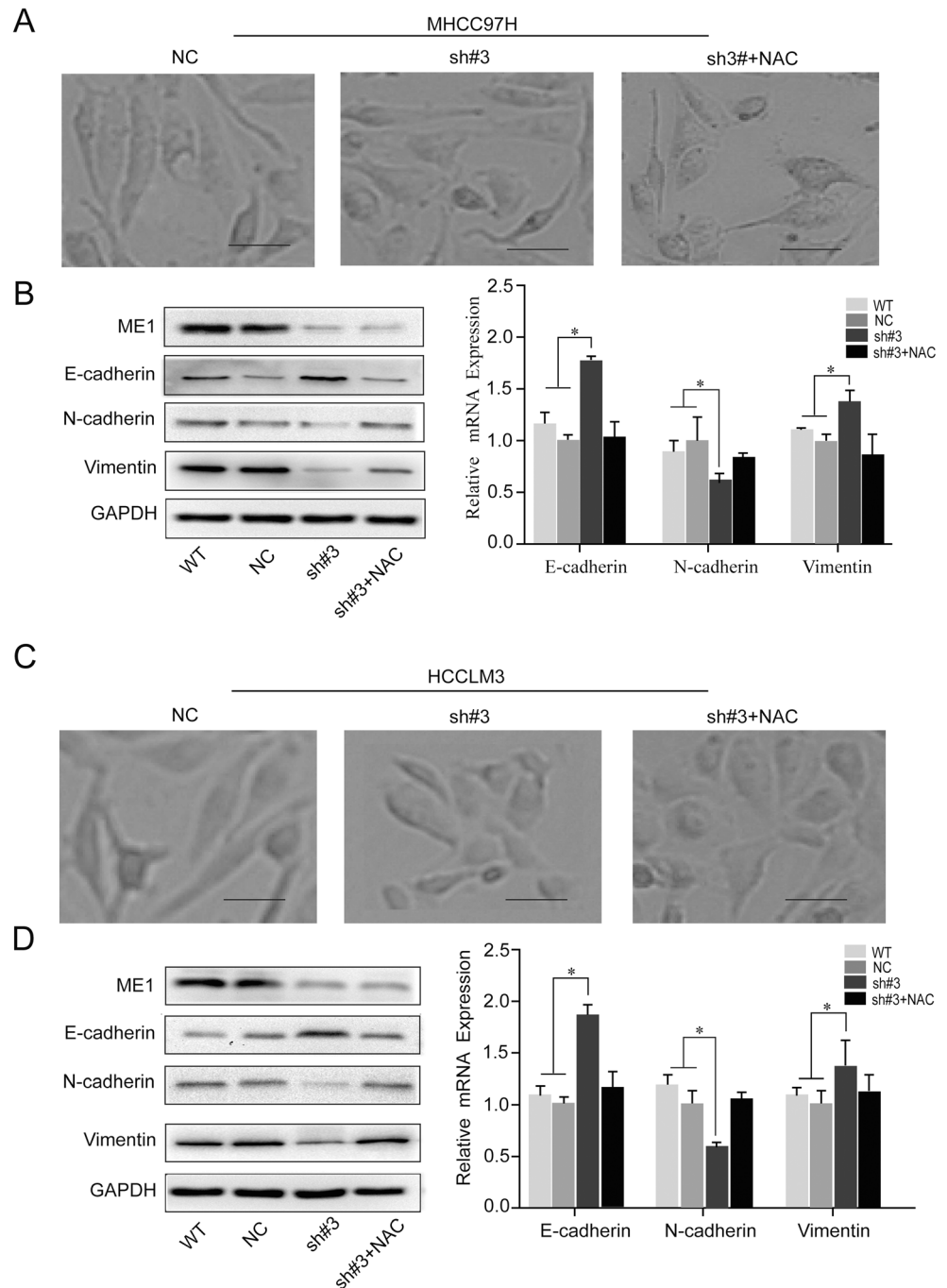
DCFH-DA probe was used to measure intracellular ROS levels. As expected, ROS levels in both ME1-repressed MHCC97H and HCCLM3 lines were increased compared to that in wild-type (WT) and negative-control (NC) cells. Moreover, the addition of dimethyl L-malate, a malic enzyme substrate, can moderately restore the intracellular NADPH levels in both ME1-repressed MHCC97H and HCCLM3 cells (Fig. 1c). As a result, the intracellular ROS levels were partially reversed after the addition of dimethyl L-malate in ME1-repressed MHCC97H and HCCLM3 cells (Fig. 2a). These results clearly demonstrate that ME1 promotes NADPH production and reduces ROS levels in HCC cells.

The inhibition of ME1 reduced migration and invasion in HCC cell lines

Next, the roles of ME1 on HCC migration and invasiveness were examined. Loss-of-function of ME1 was used by knocking down ME1 with specific shRNA (sh#3) in MHCC97H and HCCLM3 cells. The migration capabilities of MHCC97H and HCCLM3 cells were reduced by more than 2.3- and 2.8-fold, respectively, by sh#3 compared with the capabilities of control cells ($P<0.05$, Fig. 2b). Similarly, the invasive capabilities in ME1-repressed MHCC97H and HCCLM3 cells were also reduced by more than 1.8- and 2.0-fold, respectively, by sh#3 compared with the capabilities of control cells ($P<0.05$, Fig. 2c). All these results suggest that ME1 is a robust player of HCC migration.

Suppression of EMT in ME1-repressed HCC cells

A typical morphological change of MHCC97H and HCCLM3 was noted when treated with sh#3 against ME1. After a treatment for 60 h, MHCC97H and HCCLM3 cells become condensed to be a cobblestone-like morphology. The phenotypes suggest that ME1 could be involved in epithelial–mesenchymal transition (EMT) regulation in HCC cells. Therefore, three putative EMT biomarkers—E-cadherin, N-cadherin, and vimentin—were first evaluated by real-time PCR. Our results showed that the mRNA levels of E-cadherin were increased in ME1-repressed cells, while the mRNA levels of N-cadherin and vimentin were decreased. More important, our Western immunoblotting results confirmed the aforementioned mRNA changes of EMT biomarkers in both ME1-repressed HCC cells (Fig. 3).

EMT regulated by ME1 in ROS-dependent manner

In order to elucidate the underlying mechanisms of ME1-mediated EMT in HCC cells, the effects of intracellular ROS on EMT was investigated as it had been found negatively regulated by ME1. Therefore, NAC, a pharmacological inhibitor of ROS, was introduced to clear out the endogenous ROS

of HCC cells. After treatment, the epithelial phenotype of ME1-repressed HCC cells was partially reversed to the mesenchymal phenotype when combined treated with NAC. In addition, the mRNA and protein expression of E-cadherin was depressed while the expression of vimentin and N-cadherin were increased in ME1-repressed HCC cells after treated with NAC (Fig. 3b, d). These results suggest that the promoting effects of ME1 on EMT were ROS dependent.

Clinical significances of ME1 in HCC patients

To determine the clinical significances of ME1 in HCC patients, we evaluated the protein level of ME1 in para-tumor and cancerous tissues of 65 HCC patients. The clinical information of 65 enrolled patients was summarized in Table 1.

Table 1 Associations between ME1 expression and clinicopathological characteristics of HCC patients

| Characteristics	Cases (n=65)	Relative ME1 expression		P value*
		Low (n=35)	High (n=30)	
Sex				0.381
Male	61	32	29	
Female	4	3	1	
Age (year)				0.115
≤55	35	22	13	
>55	30	13	17	
AFP (μg/l)				0.250
≤400	31	19	12	
>400	34	16	18	
HBsAg				0.128
Positive	59	30	29	
Negative	6	5	1	
HBeAg				0.678
Positive	20	10	10	
Negative	45	25	20	
Tumor size (cm)				0.296
≤5 cm	17	11	6	
>5 cm	48	24	24	
Tumor number				0.408
1	25	11	14	
2	9	6	3	
3	31	18	13	
Clinical stage (BCLC)				**0.016**
A	2	1	1	
B	34	24	10	
C	29	11	19	

The numbers in bold indicate statistically significant data

N number of patients, *AFP* α-fetoprotein, *HBsAg* hepatitis B surface antigen, *HBeAg* hepatitis B e antigen, *BCLC* Barcelona Clinic Liver Cancer

*Qualitative variables were compared using Chi-squared test

Our immunohistochemistry results showed that ME1 was mainly located in the cytoplasm of liver as well as cancerous cells. The average density of ME1 protein in cancerous tissues was significantly higher than their paired adjacent non-HCC tissues (Fig. 4a). When cut off with mIOD, 35 of 65 patients (53.8 %) were categorized into ME1 high-expression group and the remaining (30/65, 46.2 %) into ME1 low-expression group. Two typical images with high or low ME1 staining in cancerous tissues were showed in Fig. 4b. The average ME1 density in the high-expression group was significantly higher than that of the low-expression group ($P<0.05$). The Kaplan–

Meier survival results revealed that a lower overall survival (Log-rank, $P=0.024$) and a reduced progression-free survival (Log-rank, $P=0.011$) were found in ME1 high-expression patients than those in ME1 low-expression ones, respectively (Fig. 4c). Furthermore, the univariate analyzed results with Cox proportional hazards regression model revealed that ME1 level, α-fetoprotein (AFP), hepatitis B surface antigen (HBsAg) (+), tumor size, and clinical stage grade were associated with overall survival (hazard ratio [HR], 1.794; i= 0.024; HR, 2.018, $P=0.007$; HR, 3.102; $P=0.041$; HR, 1.835; $P=0.047$; HR, 2.242 $P=0.002$, respectively).
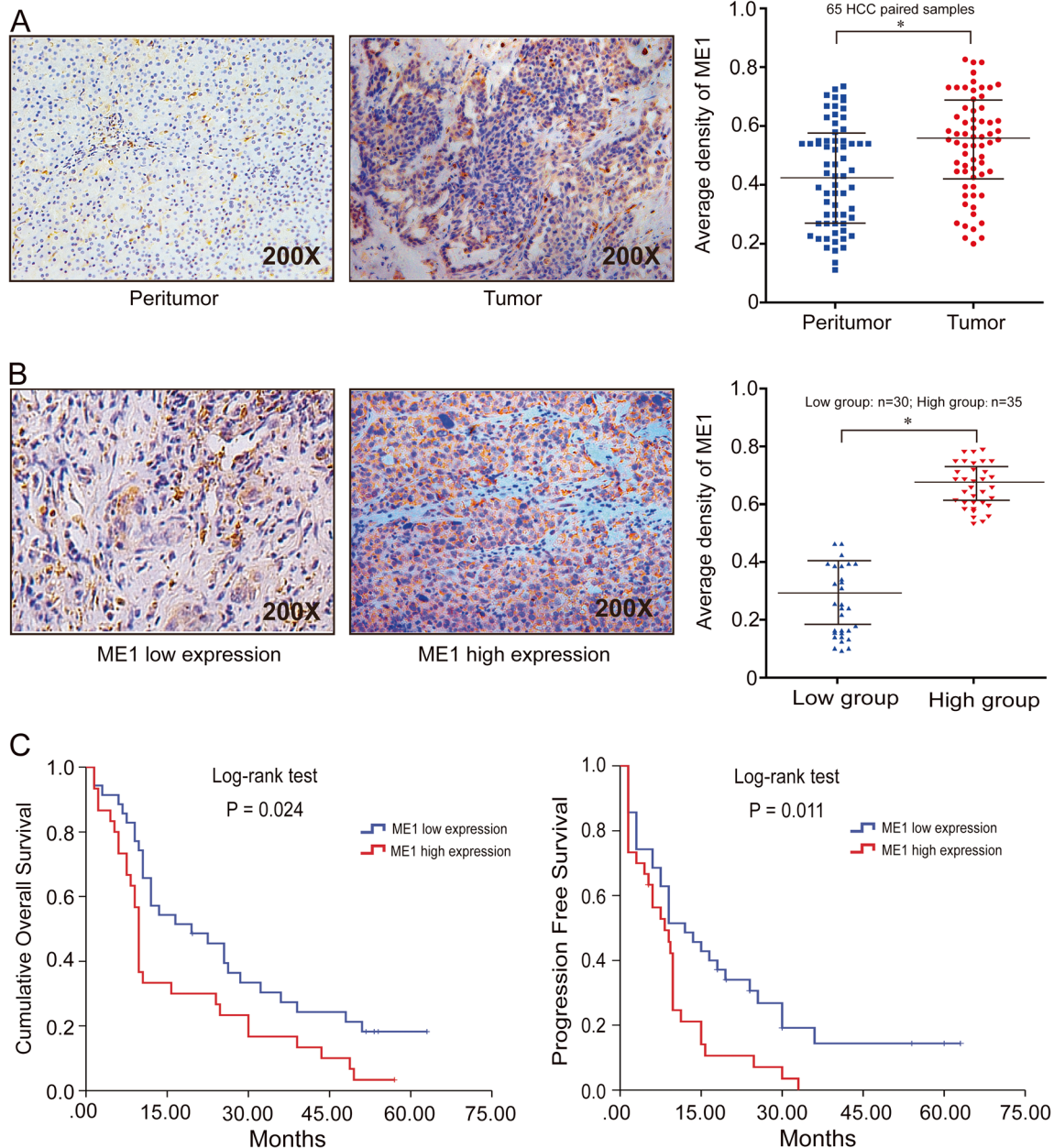
Fig. 4 Clinical validation of ME1. **a** Representative negative and positive ME1 expression in HCC tissues and their paired adjacent non-HCC tissues in immunohistochemistry (×200). **b** Representative low level and high level of ME1 expression in HCC tissues in immunohistochemistry (×200). **c** Kaplan–Meier analysis of overall survival and progression-free survival with low-level ME1 expression ($n=30$) or high-level ME1 expression ($n=65$) using SPSS 19.0. Statistical analysis by paired t test (*$P<0.05$)

Moreover, the multivariate survival analysis identified that tumor size (Table 2, HR, 1.735; P=0.042) and tumor clinical stage is the only two independent prognostic markers of HCC patients (Table 2, HR, 1.710; P=0.047). The results imply that ME1 had a moderately adverse prognosis value on HCC patients.

Discussion

The most common outcomes after HCC curative resection is tumor recurrence and metastasis. Therefore, it is deadly needed to investigate the underlying mechanisms of this metastatic disease. ME1 is reported to be a major metabolic enzyme, catalyzing the oxidative decarboxylation of malate into pyruvate and concomitantly reducing $NADP^+$ into NADPH, and by which ME1 contributes to the balance of intracellular NADPH for biological macromolecular biosynthesis and protects cells from excessive oxidative stress [9]. As the important roles of ME1 in glucose metabolism and energy production, it is ubiquitously expressed in different human tissues. In liver, ME1 is found to be moderately expressed and can be regulated by insulin and thyroid hormone [27, 28]. However, up to now, there is no research about ME1 oncological functions and its clinic significances in HCC.

In this study, we first parallel compared the ME1 levels in L02 cells with HepG2, Huh7, MHCC97L, MHCC97H, and HCCL M3 cells, and found that ME1 was expressed in all tested HCC cell lines. When ME1 was specifically suppressed by shRNA, especially of shRNA#3, the levels of intracellular NADPH were down regulated in HCC cells. This inhibitory effect after ME1 knocked-down could be partially reversed by the addition of dimethyl L-malate. All the above-mentioned results confirm that ME1 is a key regulator in NADPH in HCC cells.

Rapid growth, mitochondrial dysfunction, and increased synthesis of biological macromolecules often result in accumulation of ROS in cancerous cells. In spite of its important role as a signaling molecule [29], the excessive level of ROS can damage cytoplasmic proteins and lead cell apoptosis [30, 31]. In order to dampen this deleterious effect, ME1 was recruited to enhance NADPH production and maintain cytoplasmic redox homeostasis [32]. Indeed, silencing ME1 in MHCC97H and HCCLM3 cells was able to increase the intracellular levels of ROS. A treatment of dimethyl L-malate was able to moderately reduce the levels of ROS in ME1-repressed HCC cells due to partial restoration of NADPH production.

As tumor migration and invasiveness are two key factors on tumor progression and patients' prognosis. Naturally, we wondered if high endogenous levels of ME1, and subsequent disturbing the balances of intracellular NADPH and ROS could exert any influences on cell migration and invasiveness of HCC cells. Indeed, silencing ME1 in MHCC97H and HCCLM3 cells do inhibit the migratory and invasive capabilities in both HCC cells. More interesting, lower motility abilities were often companied with morphological changes, from mesenchymal phenotype to epithelial phenotype, in ME1-repressed HCC cells. During this process, E-cadherin level was increased while N-cadherin and vimentin levels were deceased after ME1 knockdown. The results confirm that EMT is essential for cancerous cells to acquired migratory and invasive abilities [20, 33]. Because metabolic reprogramming was reported to be involved in EMT process [7, 34, 35], and moreover, the EMT of prostate cancer cells could be regulated by ROS through TGF-β and HIF-1 signaling[36], the ROS effect on HCC EMT was evaluated using NAC, a putative robust ROS scavenger. After pretreatment with NAC, a EMT phenotype, from mesenchymal to epithelial transition,

Table 2 Univariate and multivariate survival analysis of HCC patients

Variables	Univariate analysis			Multivariate analysis		
	HR	95 % CI	P value	HR	95 % CI	P value
Sex (male, female)	1.028	0.370–2.853	0.957	1.231	0.393–3.855	0.721
Age (≤55, >55)	0.840	0.499–1.416	0.504	0.693	0.377–1.275	0.238
AFP (≤400 μg/l, >400 μg/l)	2.018	1.182–3.444	**0.007**	1.729	0.958–3.123	0.069
HBsAg (+/−)	3.102	0.967–9.955	**0.041**	2.264	0.643–7.971	0.203
HBeAg (+/−)	1.532	0.877–2.676	0.122	1.356	0.711–2.585	0.355
Tumor size (≤5, >5 cm)	1.835	0.986–3.416	**0.047**	1.735	0.759–3.702	**0.042**
Tumor number (1, 2, 3)	1.101	0.818–1.483	0.402	1.124	0.799–1.581	0.504
Clinical stage (BCLC A, B, C)	2.242	1.362–3.693	**0.002**	1.710	1.006–2.905	**0.047**
ME1(low, high)	1.794	1.061–3.033	**0.024**	1.531	0.823–2.849	0.179

The numbers in bold indicate statistically significant data

AFP α-fetoprotein, *HBsAg* hepatitis B surface antigen, *HBeAg* hepatitis B surface antigen, *+/−* positive/negative, *BCLC* Barcelona Clinic Liver Cancer, *HR* hazard ratio, *95% CI* 95 % confidence interval

was obviously induced in ME1-repressed cells accompanied by an increased E-cadherin expression as well as decreased N-cadherin and vimentin expression. The results speculate that ME1 promote HCC EMT possibly via decreasing the intracellular levels of ROS.

To further elucidate the clinical significance of ME1, the protein levels were evaluated in para-tumor and cancerous tissues of 65 HCC patients. In general, ME1 was less expressed in normal liver tissues than tumor tissues. However, ME1 expressed levels were heterogeneous in HCC tissues. HCC patients with high-expression levels had a shorter period time of overall and progression-free survival. Moreover, ME1 is an independent predictor of HCC in our univariate analysis.

In conclusion, ME1 promotes HCC migration and invasiveness, and is a poor prognostic biomarker in HCC patients. Therefore, ME1 could be a promising predictive biomarker in HCC patients, although further studies are still needed in the future.

Conflicts of interest None

Authors' Contributions D Wen, DL Liu, and WZ Wu conceived and designed the study. D Wen, DL Liu, J Tang, LL Dong, Y Liu, JL Wan, and ZH Tang performed the experiments including IHC, RT-PCR, Western blotting, and in vivo assays. D Wen, and DL Liu performed NADPH quantification assays. D Wen, DL Liu, and WZ Wu analyzed the data and prepared the manuscript. L Wang, HC Sun, and J Fan participated in the study design. All authors read and approved the final manuscript.

References

1. Mazzanti R, Gramantieri L, Bolondi L. Hepatocellular carcinoma: epidemiology and clinical aspects. Mol Asp Med. 2008;29:130–43.

2. Hu L, Xue F, Li Y, Shao M, Sun Y, Wei G. A long-term follow-up and comprehensive observation of risk and prognosis factors of recurrence and survival after resection of hepatocellular carcinoma. Cell Biochem Biophys. 2014;69:421–31. Springer US.

3. Kim J-W, Dang CV. Cancer's molecular sweet tooth and the Warburg effect. Cancer Res. 2006;66:8927–30. American Association for Cancer Research.

4. Chen Z, Wang Z, Guo W, Zhang Z, Zhao F, Zhao Y, et al. TRIM35 interacts with pyruvate kinase isoform M2 to suppress the Warburg effect and tumorigenicity in hepatocellular carcinoma. Oncogene. 2014.

5. Corominas-Faja B, Cuyàs E, Gumuzio J, Bosch-Barrera J, Leis O, Martin ÁG, et al. Chemical inhibition of acetyl-CoA carboxylase suppresses self-renewal growth of cancer stem cells. Oncotarget. 2014;5:8306–16.

6. Wang J, Yuan W, Chen Z, Wu S, Chen J, Ge J, et al. Overexpression of G6PD is associated with poor clinical outcome in gastric cancer. Tumour Biol. 2012;33:95–101. Springer Netherlands.

7. Jiang L, Xiao L, Sugiura H, Huang X, Ali A, Kuro-O M, et al. Metabolic reprogramming during TGFβ1-induced epithelial-to-mesenchymal transition. Oncogene. 2014;0.

8. Jiang L, Wang H, Li J, Fang X, Pan H, Yuan X, et al. Up-regulated FASN expression promotes transcoelomic metastasis of ovarian cancer cell through epithelial-mesenchymal transition. Int J Mol Sci. 2014;15:11539–54.

9. Wise EM, Ball EG. Malic enzyme and lipogenesis. Proc Natl Acad Sci U S A. 1964;52:1255–63.

10. Al-Dwairi A, Pabona JMP, Simmen RCM, Simmen FA. Cytosolic malic enzyme 1 (ME1) mediates high fat diet-induced adiposity, endocrine profile, and gastrointestinal tract proliferation-associated biomarkers in male mice. Singh SR, editor. PLoS ONE. Public Library of Science; 2012;7:e46716.

11. Jiang P, Du W, Mancuso A, Wellen KE, Yang X. Reciprocal regulation of p53 and malic enzymes modulates metabolism and senescence. Nature. 2013;493:689–93.

12. Zheng F-J, Ye H-B, Wu M-S, Lian Y-F, Qian C-N, Zeng Y-X. Repressing malic enzyme 1 redirects glucose metabolism, unbalances the redox state, and attenuates migratory and invasive abilities in nasopharyngeal carcinoma cell lines. Chin J Cancer. 2012;31:519–31.

13. Tang ZY, Sun FX, Tian J, Ye SL, Liu YK, Liu KD, et al. Metastatic human hepatocellular carcinoma models in nude mice and cell line with metastatic potential. World J Gastroenterol. 2001;7:597–601.

14. Li Y, Tang ZY, Ye SL, Liu YK, Chen J, Xue Q, et al. Establishment of cell clones with different metastatic potential from the metastatic hepatocellular carcinoma cell line MHCC97. World J Gastroenterol. 2001;7:630–6.

15. Pi H, Xu S, Zhang L, Guo P, Li Y, Xie J, et al. Dynamin 1-like-dependent mitochondrial fission initiates overactive mitophagy in the hepatotoxicity of cadmium. Autophagy. 2013;9:1780–800. Taylor & Francis.

16. Hu Y-J, Li H-Y, Qiu K-J, Li D-C, Zhou J-H, Hu Y-H, et al. Downregulation of Notch1 inhibits the invasion of human hepatocellular carcinoma HepG2 and MHCC97H cells through the regulation of PTEN and FAK. Int J Mol Med. 2014;34:1081–6. Spandidos Publications.

17. Sun FX, Tang ZY, Lui KD, Ye SL, Xue Q, Gao DM, et al. Establishment of a metastatic model of human hepatocellular carcinoma in nude mice via orthotopic implantation of histologically intact tissues. Int J Cancer. 1996;66:239–43. Wiley Subscription Services, Inc., A Wiley Company.

18. Li Y, Tang Z, Ye S, Liu Y, Chen J, Xue Q, et al. Establishment of human hepatocellular carcinoma cell line with spontaneous pulmonary metastasis through in vivo selection. Zhonghua Yi Xue Za Zhi. 2002;82:601–5.

19. Li Y, Tang Y, Ye L, Liu B, Liu K, Chen J, et al. Establishment of a hepatocellular carcinoma cell line with unique metastatic characteristics through in vivo selection and screening for metastasis-related genes through cDNA microarray. J Cancer Res Clin Oncol. 2003;129:43–51.

20. Tao Z-H, Wan J-L, Zeng L-Y, Xie L, Sun H-C, Qin L-X, et al. miR-612 suppresses the invasive-metastatic cascade in hepatocellular carcinoma. J Exp Med. 2013;210:789–803. Rockefeller Univ Press.

21. Xiao C-L, Tao Z-H, Guo L, Li W-W, Wan J-L, Sun H-C, et al. Isomalto oligosaccharide sulfate inhibits tumor growth and metastasis of hepatocellular carcinoma in nude mice. BMC Cancer. 2011;11:150. BioMed Central Ltd.

22. Jankowski A, Grinstein S. A noninvasive fluorimetric procedure for measurement of membrane potential. Quantification of the NADPH oxidase-induced depolarization in activated neutrophils. J Biol Chem. 1999;274:26098–104.

23. Yang Y, Parsons KK, Chi L, Malakauskas SM, Le TH. Glutathione S-transferase-micro1 regulates vascular smooth muscle cell proliferation, migration, and oxidative stress. Hypertension. 2009;54:1360–8. Lippincott Williams & Wilkins.

24. Zhu X-D, Zhang J-B, Zhuang P-Y, Zhu H-G, Zhang W, Xiong Y-Q, et al. High expression of macrophage colony-stimulating factor in

peritumoral liver tissue is associated with poor survival after curative resection of hepatocellular carcinoma. J Clin Oncol. 2008;26:2707–16. American Society of Clinical Oncology.

25. Gill JL, Bishop SC, McCorquodale C, Williams JL, Wiener P. Identification of polymorphisms in the malic enzyme 1, NADP(+)-dependent, cytosolic and nuclear receptor subfamily 0, group B, member 2 genes and their associations with meat and carcass quality traits in commercial Angus cattle. Anim Genet. 2012;43:88–92. Blackwell Publishing Ltd.

26. Rouaud F, Romero-Perez M, Wang H, Lobysheva I, Ramassamy B, Henry E, et al. Regulation of NADPH-dependent nitric oxide and reactive oxygen species signalling in endothelial and melanoma cells by a photoactive NADPH analogue. Oncotarget. 2014;5:10650–64.

27. Goodridge AG, Adelman TG. Regulation of malic enzyme synthesis by insulin triiodothyronine, and glucagon in liver cells in culture. J Biol Chem. 1976;251:3027–32.

28. Istvan ES. Structural mechanism for statin inhibition of 3-hydroxy-3-methylglutaryl coenzyme A reductase. Am Heart J. 2002;144:S27–32.

29. Wang M, Sun S, Neufeld CI, Perez-Ramirez B, Xu Q. Reactive oxygen species-responsive protein modification and its intracellular delivery for targeted cancer therapy. Angew Chem Int Ed Engl. 2014;53:13444–8. WILEY-VCH Verlag.

30. Liu-Smith F, Dellinger R, Meyskens FL. Updates of reactive oxygen species in melanoma etiology and progression. Arch Biochem Biophys. 2014;563C:51–5.

31. Wei S, Wang Y, Chai Q, Fang Q, Zhang Y, Wang J. Potential crosstalk of Ca2+−ROS-dependent mechanism involved in apoptosis of Kasumi-1 cells mediated by heme oxygenase-1 small interfering RNA. Int J Oncol. 2014;45:2373–84. Spandidos Publications.

32. Esmaeili MA, Farimani MM, Kiaei M. Anticancer effect of calycopterin via PI3K/Akt and MAPK signaling pathways, ROS-mediated pathway and mitochondrial dysfunction in hepatoblastoma cancer (HepG2) cells. Mol Cell Biochem. 2014;397:17–31. Springer US.

33. Yang M-H, Chen C-L, Chau G-Y, Chiou S-H, Su C-W, Chou T-Y, et al. Comprehensive analysis of the independent effect of twist and snail in promoting metastasis of hepatocellular carcinoma. Hepatology. 2009;50:1464–74. Wiley Subscription Services, Inc., A Wiley Company.

34. Li J, Dong L, Wei D, Wang X, Zhang S, Li H. Fatty acid synthase mediates the epithelial-mesenchymal transition of breast cancer cells. Int J Biol Sci. 2014;10:171–80.

35. Liu Y, Liu Y, Yan X, Xu Y, Luo F, Ye J, et al. HIFs enhance the migratory and neoplastic capacities of hepatocellular carcinoma cells by promoting EMT. Tumour Biol. 2014;35:8103–14. Springer Netherlands.

36. Das TP, Suman S, Damodaran C. Induction of reactive oxygen species generation inhibits epithelial–mesenchymal transition and promotes growth arrest in prostate cancer cells. Mol Carcinog. 2014;53:537–47.